Journal of
MASS SPECTROMETRY

Received: 23 December 2011 Revised: 10 February 2012 Accepted: 11 February 2012

(wileyonlinelibrary.com) DOI 10.1002/jms.2977

A '*meta* effect' in the fragmentation reactions of ionised alkyl phenols and alkyl anisoles

Guy Bouchoux,[a]* Michel Sablier,[a] Tetsuo Miyakoshi[b] and Takashi Honda[b]

The competition between benzylic cleavage (simple bond fission [SBF]) and retro-ene rearrangement (RER) from ionised *ortho*, *meta* and *para* RC_6H_4OH and $RC_6H_4OCH_3$ ($R = n\text{-}C_3H_7$, $n\text{-}C_4H_9$, $n\text{-}C_5H_{11}$, $n\text{-}C_7H_{15}$, $n\text{-}C_9H_{19}$, $n\text{-}C_{15}H_{31}$) is examined. It is observed that the SBF/RER ratio is significantly influenced by the position of the substituent on the aromatic ring. As a rule, phenols and anisoles substituted by an alkyl group in *meta* position lead to more abundant methylene-2,4-cyclohexadiene cations (RER fragmentation) than their *ortho* and *para* homologues. This '*meta* effect' is explained on the basis of energetic and kinetic of the two reaction channels. Quantum chemistry computations have been used to provide estimate of the thermochemistry associated with these two fragmentation routes. G3B3 calculation shows that a hydroxy or a methoxy group in the *meta* position destabilises the SBF and stabilises the RER product ions. Modelling of the SBF/RER intensities ratio has been performed assuming two single reaction rates for both fragmentation processes and computing them within the statistical RRKM formalism in the case of *ortho*, *meta* and *para* butyl phenols. It is clearly demonstrated that, combining thermochemistry and kinetics, the inequality $(SBF/RER)_{meta} < (SBF/RER)_{ortho} < (SBF/RER)_{para}$ holds for the butyl phenols series. It is expected that the '*meta* effect' described in this study enables unequivocal identification of *meta* isomers from *ortho* and *para* isomers not only of alkyl phenols and alkyl anisoles but also in other alkyl benzene series. Copyright © 2012 John Wiley & Sons, Ltd.

Keywords: electron ionisation; substituted alkyl benzenes; fragmentation competition; retro-ene rearrangement; benzylic cleavage; quantum chemistry computation; RRKM modelling

INTRODUCTION

Competitions between simple bond fission (SBF) and rearrangement are ubiquitous events in gas phase ion chemistry.[1] Prototypes of such competition are the allylic cleavage/retro-ene fragmentations of ionised alkenes and the homologue benzylic cleavage/retro-ene fragmentations of ionised alkyl benzenes (Scheme 1).

In this latter series, the two competitive channels are (i) the C–C bond elongation leading to the benzyl cation (*m/z* 91 in Scheme 1) plus a *n*-propyl radical (SBF fragmentation, Scheme 1) and (ii) the retro-ene rearrangement (RER) producing ionised methylene-2,4-cyclohexadiene (*m/z* 92 in Scheme 1) and propene (RER fragmentation, Scheme 1). Probably the most extensively studied example of competition between SBF and RER fragmentations during the last decades is ionised butyl benzene.[2–22] Experiments on this system involved ion-beam[2,3,6,8,9] and trapped-ion[4] photodissociation, charge exchange ionisation,[10,11] collisional activation,[11–14] chemical and thermal activation[15] and photoelectron–photoion coincidence technique.[7] These experiments allowed to explore a range of internal energy, *E*, of the butyl benzene molecular ion extending from ~2 to ~6 eV. A strong dependence of the ratio of ion abundances [*m/z* 91]/[*m/z* 92] with internal energy *E* has been observed and quantitatively ascertained thus leading to call the butyl benzene radical cation a 'thermometer ion'. For this type of competition, the SBF fragmentation is usually characterised by a high critical energy and a loose transition structure while the RER fragmentation passes through a more congested transition structure but presents a lower critical energy. As a consequence, the two rate constants associated with these fragmentations exhibit a crossing point. Under these circumstances, it is understandable why the ratio of peak intensities [*m/z* 91]/[*m/z* 92] passes from zero at low internal energy *E* to a value significantly higher than unity at high *E* values for butyl benzene.

If the cases of alkyl benzenes are well described, less information is available on substituted alkyl benzenes where competition between SBF and RER may be influenced by the nature of the substituent and by its position relative to the alkyl chain on the aromatic ring. In the present study, we explore the fragmentation patterns of molecular cations produced by electron ionisation of *ortho*, *para* and *meta* substituted alkyl phenols and alkyl anisoles. It will be shown that it is possible to distinguish the substitution sites in these series by using the SBF/RER ratio, in particular a '*meta* effect' is evidenced. An explanation of the experimental observation is provided by examining the fragmentation energetic of the two competitive reactions channels using quantum chemical computation and by modelling the reaction kinetic using statistical rate calculations to take into account internal energy and entropy effects.

EXPERIMENTAL AND COMPUTATIONAL SECTION

Computational details

Quantum chemistry calculations have been conducted using the GAUSSIAN03 suite of programs[23] within the density functional

---

* *Correspondence to: Guy Bouchoux, DCMR, Ecole Polytechnique, 91128, Palaiseau Cedex, France. E-mail: bouchoux@dcmr.polytechnique.fr*

a *Laboratoire des Mécanismes Réactionnels, Ecole Polytechnique, CNRS, 91128 Palaiseau, France*

b *School of Science and Technology, Meiji University, Higashi-Mita 1-1-1, Tama-ku Kawasaki, 214-8571, Japan*

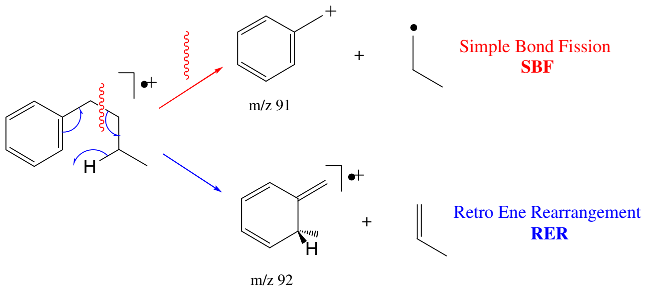

Scheme 1. Competition between simple bond fission (SBF) and retro-ene rearrangement (RER).

theory. Geometries were optimised at the B3LYP/6-31 + G(d,p) level of theory, and unscaled vibrational frequencies calculated at this level were used to calculate vibrational contribution to enthalpy at 0 K and 298 K. Although geometrical parameters are well reproduced at this level of theory, limitations of B3LYP/6-31 + G(d,p) computations to evaluate precise reaction energies or heats of formation were documented in recent reviews.[24] Means to correct for these deficiencies consist to perform single point energy calculations with enlarged basis set or(and) with different correlated methods. A popular procedure, which was applied to the various systems examined here, uses a simple extension of the basis set size such as B3LYP/6-311++G(3df,2p)//B3LYP/6-31 + G(d,p) single point calculation. A second possibility involves more expensive composite methods such as the Gn procedures. We used here the G3B3 composite method[25] to estimate several crucial heats of formation values.

GC/MS analytical conditions

The gas chromatography/mass spectrometry measurements were carried out using an Agilent 6890 N/5975 GC/MS system (Agilent tec., Ltd). The samples of 2-alkyl phenol (1) and 3-alkyl phenol (2) were dissolved in acetone (4.0 mg in 1 ml). Approximately 1 μl of each solution was injected in the stainless steel capillary column (0.25 mm i.d. × 30 m) coated with Ultra Alloy PY-1(HT/MS) (100% methyl silicone) of the gas chromatograph. The gas chromatograph oven was programmed to provide a constant temperature increase of 12 °C per min from 40 °C to 320 °C then held for 10 min at 320 °C. The injection and the interface temperatures were equal to 280 °C. The flow rate of helium gas was 1 ml/min. All products were identified by mass spectrometry in the electron ionisation mode (EI-mode) using ionisation energy of 70 eV.

Synthesis of alkyl phenols and alkyl anisoles

One of us previously developed efficient method for synthesising urushiol analogues.[26] In the present study, this experimental procedure has been followed to synthesise *ortho* and *meta* substituted alkyl phenols and alkyl anisoles using Grignard reagents. Briefly, the cross-coupling reaction of 2-anisylmagnesium bromide with alkyl bromide in presence of copper (I) chloride in THF gave 2-alkyl anisoles in 75% to 86% yields[27]:

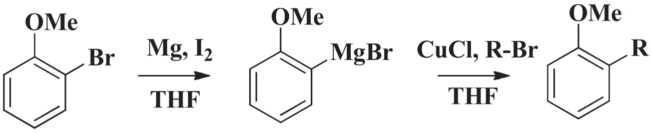

Demethylation of 2-alkyl anisoles with BBr_3 in $CHCl_3$ gives the corresponding 2-alkyl phenols in ~95% yields[28]:

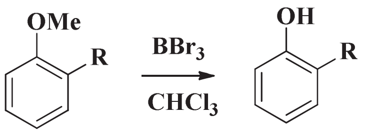

Starting with 3-anisyl bromide, similar reactions provide 3-alkyl anisoles and 3-alkyl phenols.[29]

RESULTS AND DISCUSSION

Experimental evidence for a meta effect

The 70-eV electron ionisation mass spectra of *ortho* and *meta* substituted alkyl phenols and alkyl anisoles synthetised as described earlier were recorded, and the essential data are presented in Table 1 together with some previous literature results.[30] The SBF and the RER reactions (Scheme 1) cause *m/z* 107 and 108 fragment ions in the case of alkyl phenols, and these signals are obviously displaced to *m/z* 121 and 122 for alkyl anisoles.

An essential observation that emerges from examination of Table 1 is that the SBF/RER ratio is always lower for the *meta* isomers than for the *ortho* or *para* counterparts for a given side chain length. Thus, the *meta* substituted alkyl phenols and alkyl anisoles exhibit a distinct behaviour allowing us to speak of a '*meta* effect'. The data presented in Table 1 also show that the ratio SBF/RER decreases markedly when the number of carbon atoms of the alkyl chain increases from C_3 to C_5 until attaining a constant limiting value of ~ 0.5 (0.3) for *meta* and ~7 (22) for *ortho* hydroxyl (methoxy) isomers as illustrated on Fig. 1. Note that the few examples of *para* isomers closely follow the *ortho* behaviour.

To understand the origin of this *meta* effect on the fragmentations of ionised alkyl phenols and alkyl anisoles, we first examined the thermochemistry of these reactions using both known thermochemical data and quantum chemistry calculations. Because it will be seen that thermochemistry is insufficient to explain the experimental observations, a reaction rates modelling on the basis of the butyl benzene case has been further undertaken to include internal energy effect.

Theoretical results: thermochemistry

The thermochemistry of the SBF and RER reaction products of alkyl benzene, alkyl phenols and alkyl anisoles bearing an alkyl chain ranging from C_3 to C_9 is summarised in Tables 2 and 3. The difference in enthalpies between the two sets of fragmentation products, $\Delta H^\circ_{\text{SBF-RER}} = \Sigma\ \Delta_f H^\circ(\text{SBF products}) - \Sigma\ \Delta_f H^\circ(\text{RER products})$, is presented in Table 3. The corresponding values were determined using the individual 298 K heats of formations computed using the atomisation energies obtained at the G3B3 level of theory (Table 2).

The general feature, underlined in the Introduction section, of a larger endothermicity of the SBF with respect to the rearrangement is clearly apparent in Table 3. For all the alkyl benzenes and alkyl phenols and all but one alkyl anisoles examined here, the term $\Delta H^\circ_{\text{SBF-RER}}$ is positive. Moreover, $\Delta H^\circ_{\text{SBF-RER}}$ seems to be only slightly influenced by the length of the alkyl chain. According to the data reported in Table 3, a noticeable increase in $\Delta H^\circ_{\text{SBF-RER}}$ is observed when passing from the propyl to the butyl benzene series. However, increasing the chain length above C_4 does not

Table 1. Competition between SBF and RER in a 70-eV electron ionisation mass spectra of some alkyl benzene derivatives XC_6H_4R

X	R		SBF%[a]	RER%[a]	RER%$_{corr}$[b]	SBF/RER$_{corr}$[b]
H	*$n\text{-}C_3H_7$*		*100*	*10*	*2.3*	*43 ± 24*
	$n\text{-}C_4H_9$		*100*	*54.6*	*46.9*	*2.1 ± 0.3*
	$n\text{-}C_5H_{11}$		*100*	*72*	*64.3*	*1.6 ± 0.2*
	$n\text{-}C_7H_{15}$		*100*	*89.5*	*81.8*	*1.2 ± 0.2*
OH	$n\text{-}C_3H_7$	*ortho*	100	10	2.3	43 ± 24
		meta	100	49	41.3	2.4 ± 0.3
		para	100	9	1.3	77 ± 70
	$n\text{-}C_4H_9$	*ortho*	100	12.8	5.1	19.6 ± 5.8
		meta	53	100	95.9	0.60 ± 0.06
		para	100	10	2.3	43 ± 24
	$n\text{-}C_5H_{11}$	*ortho*	*100*	*22*	*14.3*	*7.0 ± 1.2*
		meta	*45*	*100*	*96.5*	*0.50 ± 0.05*
		para	*100*	*15*	*7.3*	*13.7 ± 3.2*
	$n\text{-}C_7H_{15}$	*ortho*	100	22.9	15.2	6.6 ± 1.1
		meta	36.4	100	97.2	0.37 ± 0.04
	$n\text{-}C_9H_{19}$	*ortho*	100	33.2	25.5	3.9 ± 0.6
		meta	52.7	100	95.9	0.55 ± 0.06
	$n\text{-}C_{15}H_{31}$	*ortho*	100	18.5	10.8	9.3 ± 1.8
		meta	39.7	100	96.9	0.41 ± 0.05
OCH_3	$n\text{-}C_3H_7$	*ortho*	100	9.2	1.5	67 ± 53
		meta	100	83.6	75.9	1.3 ± 0.2
	$n\text{-}C_4H_9$	*ortho*	100	13.3	5.6	17.9 ± 5.0
		meta	32.9	100	97.5	0.30 ± 0.04
	$n\text{-}C_5H_{11}$	*ortho*	*100*	*12*	*4.3*	*23.3 ± 7.8*
		meta	*36*	*100*	*97.2*	*0.40 ± 0.04*
		para	*100*	*10*	*2.3*	*43 ± 24*
	$n\text{-}C_7H_{15}$	*ortho*	100	12	4.3	23.3 ± 7.8
		meta	29.5	100	97.7	0.30 ± 0.03
	$n\text{-}C_9H_{19}$	*ortho*	100	12.8	5.1	19.6 ± 5.8
		meta	31.2	100	97.6	0.30 ± 0.04
	$n\text{-}C_{15}H_{31}$	*ortho*	100	12.4	4.7	21.3 ± 6.7
		meta	33.4	100	97.4	0.30 ± 0.04
	CH_2CH_2OH	*ortho*	*100*	*23*	*15.3*	*6.5 ± 1.1*
		meta	*100*	*61*	*53.3*	*1.9 ± 0.2*
NH_2	*$n\text{-}C_6H_{13}$*	*ortho*	*100*	*14.9*	*7.2*	*13.9 ± 3.3*
		meta	*37.2*	*100*	*97.1*	*0.40 ± 0.04*
		para	*100*	*9.1*	*1.4*	*71 ± 61*

[a] In italic, from NIST mass spectra database.[30]

[b] Corrected for the ^{13}C contribution of the SBF signal to the RER ion abundances. Error calculated assuming 10% relative error on the measured peak intensities.

change anymore this enthalpy difference. This observation parallels that of a limiting SBF/RER ratio value when the alkyl chain of phenols or anisoles is larger than C_4 as observed in Fig. 1.

The essential observation from Table 3 is certainly the clear increase in the difference in enthalpies $\Delta H^\circ_{\text{SBF-RER}}$ when passing from *para* to *ortho* and to *meta* isomers for phenols or anisoles of a given alkyl chain length. It is noteworthy that $\Delta H^\circ_{\text{SBF-RER}}$ is as high as 85–100 kJ/mol for the *meta* isomers, whereas it never exceeds 20 or 50 kJ/mol for its *para* and *ortho* counterparts. We chose, as a representative example, the case of *ortho*, *meta* and *para* ionised butyl phenols to illustrate this behaviour. This system was investigated at the B3LYP/6-311++G(3df,2p)//B3LYP/6-31 + G(d,p) level of theory. The resulting 0 K energy profiles associated with SBF and RER fragmentations of these molecular cations are presented in Fig. 2. At the B3LYP/6-311++G(3df,2p)//B3LYP/6-31 + G(d,p) level, the 0 K $\Delta H^\circ_{\text{SBF-RER}}$ values are equal to 19, 48 and 98 kJ/mol for *para*, *ortho* and *meta* isomers, respectively (values that compare closely with the 298 K G3B3 computed $\Delta H^\circ_{\text{SBF-RER}}$ of 20, 50 and 99 kJ/mol; Table 3).

The origin of the clear influence of the substitution site, evidenced in Fig. 2 for butyl phenols and in Table 3 for a larger panel of molecules, is obviously that the stabilities of the SBF and RER fragment ions are strongly influenced by the position of the hydroxyl group. More specifically, the benzyl cation is stabilised by OH (or OCH_3) group in position *para* or *ortho* while, by contrast, ionised methylene-2,4-cyclohexadiene is more stable when the hydroxyl (or methoxy) group is in position *meta*. Insight on these questions is provided by quantum chemistry calculations of charge and spin densities.

Natural bond orbital and Atomic Polar Tensor population analysis show that, as expected, benzyl cation may be described by the four canonical forms A, B, C and C′ (Scheme 2).[31]

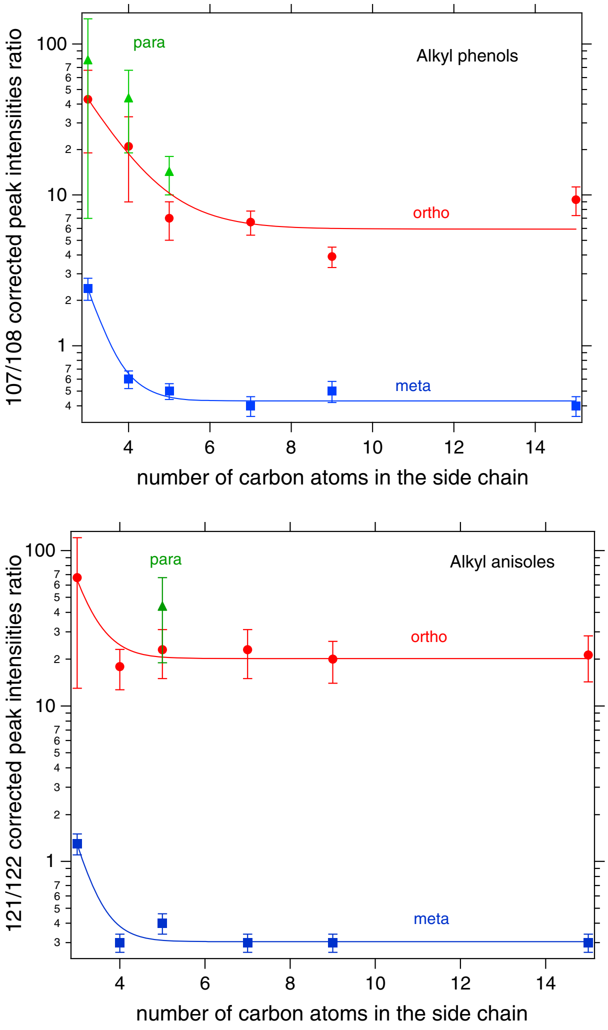

Figure 1. SBF/RER ratio as a function of the alkyl chain length for substituted phenols (up) and substituted anisoles (down).

Consequently, substitution by a π-donor group in position *para* or *ortho* would provide a significant stabilisation to the corresponding species. This is indeed what is observed when the computed $\Delta_fH°$ of the three hydroxy benzyl cations are considered (Table 2). At 298 K, the *para* and *ortho* hydroxy benzyl cations are more stable than their *meta* homologue by 53 and 34 kJ/mol, respectively (G3B3 calculations[32]; Table 2). Similar $H°_{298}$ differences of 52 and 39 kJ/mol are observed for the methoxy derivatives (Table 2).

Concerning ionised methylene-2,4-cyclohexadiene, Mulliken population analysis shows a major spin density on the carbon atom of the exocyclic methylene (**I**, Scheme 3) and a minor contribution on carbon C(5) (**II**, Scheme 3). Therefore, the set of canonical forms **I** would mainly describe the electronic configuration of this radical cation (Scheme 3). Considering the two electronic structures **IA** and **IB**, it is evident that the presence of an OH group in positions C(3) (*meta*) or C(5) (*meta'*) would stabilise the radical cation. Accordingly, the two hydroxy 2,4-cyclohexadiene substituted by the OH group in positions C(3) and C(5) are indeed more stable than their homologues *ortho* and *para* (by 15 and 26 kJ/mol, respectively, G3B3 calculations[32]; Table 2). Comparable gain in stability is obtained for the methoxy homologues (17 and 34 kJ/mol, respectively, G3B3 calculations, Table 2).

Theoretical results: kinetic modelling of reactions rates.

According to the data presented in Fig. 2 and in Table 3, it would be tempting to predict that the RER fragmentation should be always dominant because, whatever the substitution site, it is the process of lower energy. This is in conflict with the fact that the SBF fragmentation is dominant in the 70-eV mass spectra of *para* and *ortho* alkyl phenols and alkyl anisoles. Thermochemistry alone is consequently unable to explain the experimental observations. Consideration of the nature of the transition structure and of the internal energy effect on SBF and RER reaction rates is consequently essential to understand the clear-cut character of the observed *meta* effect. For this purpose, we performed statistical modelling of the reaction kinetics on the *ortho*, *meta* and *para* butyl

Table 2. Heats of formation ($\Delta_fH_{298}°$)[a] of the various species involved in the SBF and RER fragmentations of alkyl benzene, alkyl phenols and alkyl anisoles (kJ/mol)

Species	H	OH		OCH$_3$	
Benzyle$^+$	912.7	*ortho*	699[b]	*ortho*	700
		meta	733[b]	*meta*	739
		para	680[b]	*para*	681
Methylene-2,4-cyclohexadiene $^{\cdot+}$	947.4	*ortho*	732[b]	*ortho*	741
		meta	717[b]	*meta*	724
		para	743[b]	*para*	758
$^{\cdot}C_2H_5$	120.6				
C_2H_4	51.5				
$n\text{-}^{\cdot}C_3H_7$	103.5				
$CH_3CH{=}CH_2$	20.0				
$n\text{-}^{\cdot}C_4H_9$	81.9				
$CH_3CH_2CH{=}CH_2$	0.4				
$n\text{-}^{\cdot}C_6H_{13}$	40.1				
$CH_3(CH_2)_3CH{=}CH_2$	−42.0				
$n\text{-}^{\cdot}C_8H_{17}$	−1.9				
$CH_3(CH_2)_5CH{=}CH_2$	−84.1				

[a] G3B3 calculations using atomisation energies.
[b] From Bouchoux.[32]

Table 3. Enthalpy differences (kJ/mol) between SBF and RER products originating from competitive fragmentations of ionised benzene derivatives XC_6H_4R (G3B3 computations)

X	R			$\Delta H°^{a}_{SBF\text{-}RER}$
H	$n\text{-}C_3H_7$			34
	$n\text{-}C_4H_9$			49
	$n\text{-}C_5H_{11}$			47
	$n\text{-}C_7H_{15}$			48
	$n\text{-}C_9H_{19}$			47
OH		$n\text{-}C_3H_7$	*ortho*	36
			meta	85
			para	7
		$n\text{-}C_4H_9$	*ortho*	50
			meta	99
			para	20
		$n\text{-}C_5H_{11}$	*ortho*	48
			meta	97
			para	19
		$n\text{-}C_7H_{15}$	*ortho*	50
			meta	99
			para	19
		$n\text{-}C_9H_{19}$	*ortho*	49
			meta	98
			para	19
OCH_3		$n\text{-}C_3H_7$	*ortho*	28
			meta	84
			para	−8
		$n\text{-}C_4H_9$	*ortho*	43
			meta	99
			para	7
		$n\text{-}C_5H_{11}$	*ortho*	41
			meta	97
			para	5
		$n\text{-}C_7H_{15}$	*ortho*	41
			meta	97
			para	5
		$n\text{-}C_9H_{19}$	*ortho*	41
			meta	97
			para	5

[a] $\Delta H°_{SBF\text{-}RER} = \Sigma\, \Delta_f H°(\text{SBF products}) - \Sigma\, \Delta_f H°(\text{RER products})$, individual G3B3 $\Delta_f H_{298}$ taken from Table 2.

phenol series using the 0 K enthalpy profiles presented in Fig. 2. Before presenting the results of this investigation, it is important to recall the major characteristics of the competitive fragmentations of ionised butyl benzene itself.

As indicated in the Introduction section, the ratio of ion abundances [91]/[92] (i.e. SBF/RER) originating from butyl benzene radical cation has been determined precisely as function of internal energy by a variety of techniques. A graphical representation of these essential data is reported in Fig. 3a. It is noteworthy that in the electron ionisation (70 eV) mass spectrum of butyl benzene, the ratio [91]/[92] is equal to 2.1, thus pointing to an average internal energy centred around 4.6 eV for this system (value indicated by a vertical bar in Fig. 3a). Photoelectron/photoion coincidence experiments on two different apparatus[7] provided rate constant $k(92)$ values between 10^5 and $10^6\,s^{-1}$, whereas photodissociation mass analysed ion kinetic energy spectroscopy was used to explored the $10^8\,s^{-1}$ region.[8] These two sets of experimental rate constant, $k(92)$, values cover a range of internal energy E situated between 2 and 5 eV. Obviously, using these data and assuming that the [91]/[92] ion abundances ratio is equal to the reaction rates ratio, one may also deduce experimental $k(91)$ values as a function of E (markers in Fig. 3b). These experimental results have been used in several kinetic modelling studies using single rate coefficient for each, m/z 91 and 92, fragmentation routes, the critical energy $E°$ of each process being treated as an adjustable parameter but generally approaching the corresponding endothermicities of the fragmentations.[7,8,14,15,22] Figure 3b

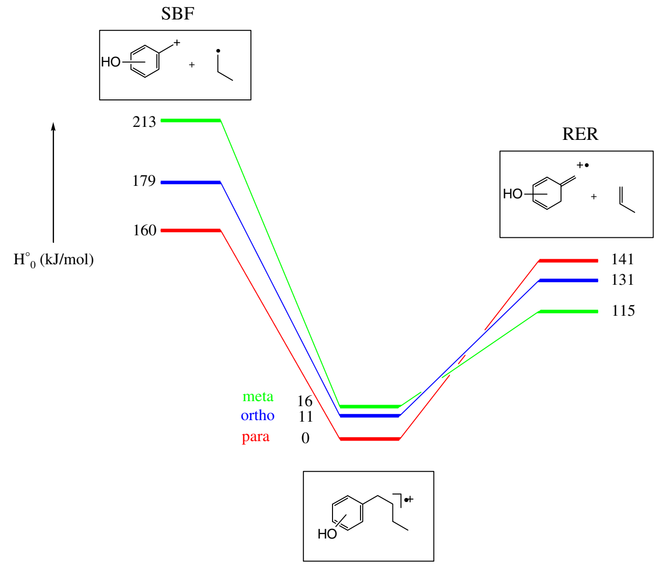

Figure 2. Zero Kelvin energy profiles for SBF and RER fragmentations of *ortho*, *meta* and *para* butyl phenols (B3LYP/6-311++G(3df,2p)//B3LYP/6-31 + G(d,p) calculations).

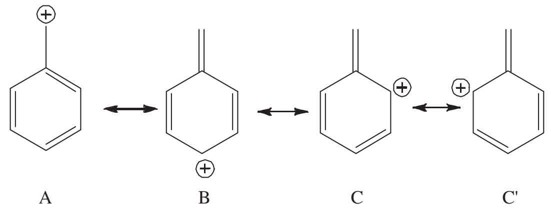

Scheme 2. Canonical forms describing benzyl cation.

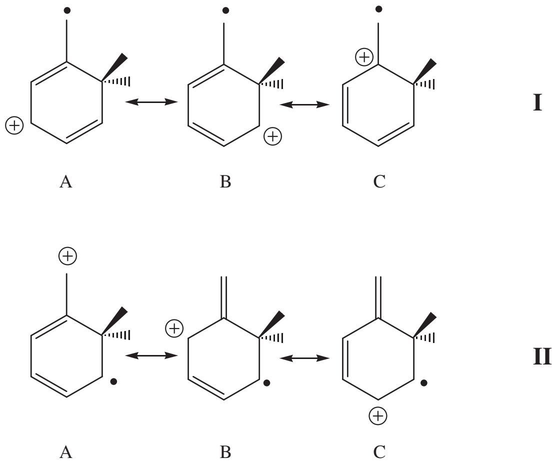

Scheme 3. Canonical forms describing methylene-2,4-cyclohexadiene radical cation.

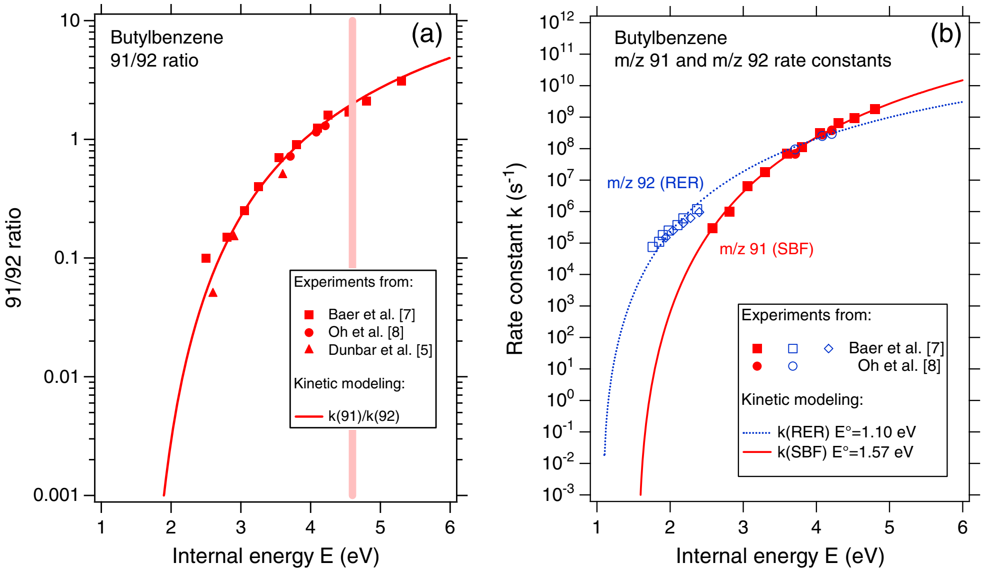

Figure 3. Experimental [*m/z* 91]/[*m/z* 92] ratio (a) and overall rate constants *k*(91) and *k*(92) (b) versus internal energy of butyl benzene molecular ion.[5,7,8] The fitting curves are obtained after kinetic modelling of *k*(91) and *k*(92).[7,8,14,21,22] Vertical bar in panel a corresponds to the average internal energy of molecular ions formed by a 70-eV electron ionisation.

presents one example of this kinetic modelling obtained using the statistical RRKM formalism and $E^\circ = 1.10$ and 1.57 eV to model *k*(92) and *k*(91) reaction rates, respectively. Figure 3b illustrates clearly the fact that the SBF fragmentation presents a high critical energy and a loose transition structure whereas the RER fragmentation possesses a low critical energy but passes through a tight transition structure. The combination of these characteristics results in the crossing of the two rate constants associated with these fragmentations and explain why the *m/z* 92 signal decreases dramatically with respect to *m/z* 91 when increasing internal energy.

It should be underlined that more sophisticated statistical rate treatment[15,21] or consideration of more complete mechanistic scheme[22] does not fundamentally alter the overall results illustrated by Fig. 3, particularly for internal energy higher than ~3 eV. Thus, we decided to extend the statistical kinetic treatment used for butyl benzene to *ortho*, *meta* and *para* butyl phenols. A modelling of the SBF/RER intensities ratio has been performed assuming two single reaction rates for both processes and computing them within the statistical RRKM formalism exactly as already performed for butyl benzene itself.[7,8,14] The essential parameters necessary for these calculations are the vibrational frequencies of the reactants and transitions states as well as the critical energies. To compute the rate constants *k*(107) and *k*(106) corresponding to SBF and RER fragmentations of butyl phenols, we used frequencies calculated at the B3LYP/6-31 + G(d,p) level for the molecular ions. Modification of some of these vibrational frequencies based on previous treatments of ionised butyl benzene[7,8,14,22] allowed us to describe the transition structures. For the SBF reaction, a C–C stretching mode (900 cm^{-1}) has been taken as reaction coordinate, and four deformation modes were reduced by a factor two and one torsional mode becomes a free rotation. Concerning the RER fragmentation, a C–H stretching mode (3100 cm^{-1}) has been taken as reaction coordinate, and six deformations and internal rotations modes were increased to reproduce the tight character of this transition structure. Finally, the critical energy values used in the rate constant calculations were the 0 K endothermicities of each fragmentation computed at the B3LYP/6311++G(3df,2p)//B3LYP/6-31 + G(d,p) + ZPE level (Fig. 2). Results obtained using this approach, in the 0- to 6-eV internal energy range, are summarised in Figs 4 and 5.

Figure 4 illustrates the SBF and the RER rate constants evolutions with internal energy for the three isomers *ortho*, *meta* and *para*

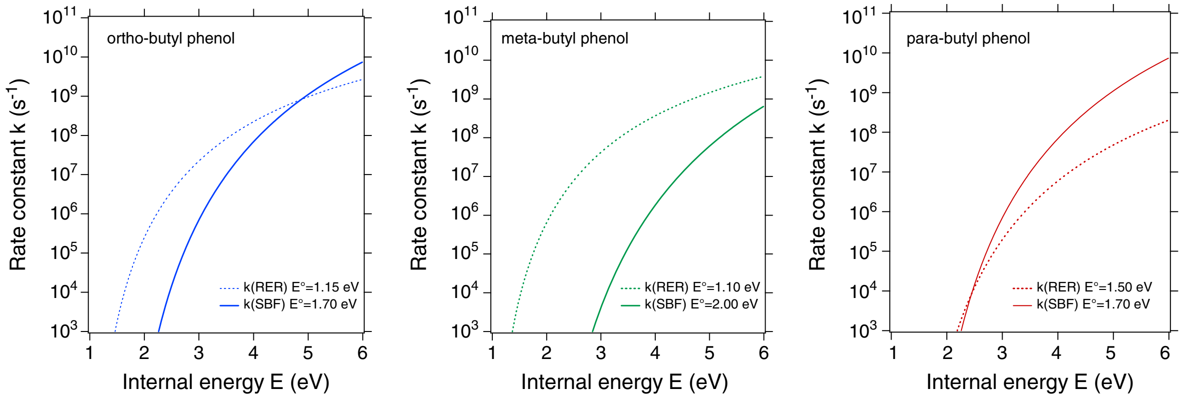

Figure 4. Individual rate constants calculated for the SBF and RER fragmentations of *ortho*, *meta* and *para* butyl phenols (using B3LYP/6-311++G(3df,2p)//B3LYP/6-31 + G(d,p) critical energies (E°), and B3LYP/6-31 + G(d,p) vibrational frequencies).

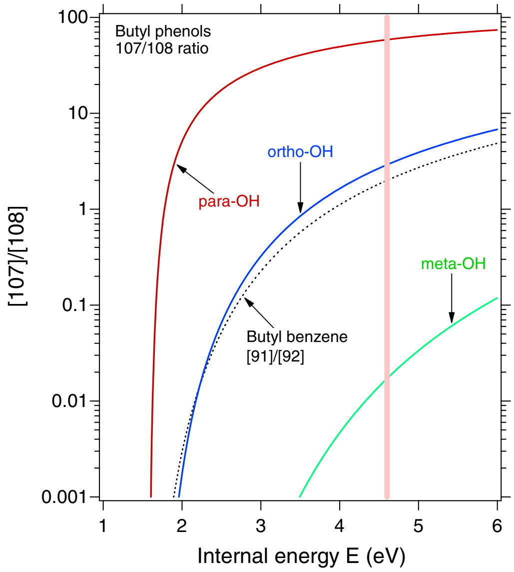

Figure 5. Calculated ratio *k*(107)/*k*(108) for *ortho*, *meta* and *para* butyl phenols and *k*(91)/*k*(92) of butyl benzene itself versus internal energy of the molecular ions. The vertical bar corresponds to the expected average internal energy of molecular ions formed by a 70-eV electron ionisation.

butyl phenols. By comparing Figs 3b and 4, we observed that *ortho* butyl phenol and butyl benzene itself behaves similarly because the two *k*(E) curves associated with SBF and RER fragmentations intercept at an internal energy *E* close to 4–5 eV. The situation is different for the *meta* isomer for which the crossing point is situated at internal energy well higher than 6 eV. Finally, the *para* isomer presents the opposite situation with a crossing point close to 2 eV. In other words, in the studied internal energy range, *k*(RER) is larger than *k*(SBF) for *meta* butyl phenol whereas the reverse is true for *para* butyl phenol, the *ortho* butyl phenol offering an intermediate situation. Another angle of view is offered by Fig. 5 where the SBF/RER ratio is plotted against the internal energy of the parent ions. A rapid increase of the SBF/RER ratio with internal energy appears clearly for the *para* and *ortho* isomers of butyl phenol. This evolution is less marked for *meta* butyl phenol. Assuming that, at 70 eV, the average internal energy is close to that of butyl benzene itself, that is ~4.6 eV, it is evident that the inequality $(\mathrm{SBF/RER})_{\mathrm{meta}} < (\mathrm{SBF/RER})_{\mathrm{ortho}} < (\mathrm{SBF/RER})_{\mathrm{para}}$ holds for the butyl phenols series. Moreover, it should be underlined that the ratio $(\mathrm{SBF/RER})_{\mathrm{meta}}$ is less than unity; that is, the retro-ene fragmentation dominates over the SBF. These conclusions are in excellent agreement with the experimental observations reported in Table 1 and in Fig. 1.

CONCLUSION

A *meta* effect is evidenced in the fragmentation reactions of ionised alkyl phenols and alkyl anisoles. For these regio-isomers, it is indeed observed that the RER is dramatically favoured over the simple benzylic bond fission (SBF). The reverse situation is observed for *ortho* and *para* isomers that behave similarly. An explanation of this phenomenon is based on a combined role of thermochemistry and kinetics. The role of π-donor substituents such as OH and OCH_3 in the *meta* position is to destabilise the SBF and to stabilise the RER products. However, it is found that whatever the substituent position, the RER fragmentation is always thermodynamically favoured over the SBF reaction, and thus thermochemistry alone is not sufficient to interpret the data. Because the SBF fragmentation is characterised by a loose transition structure, its rate constant may overcome that of the RER fragmentation at high energy. This is so for *ortho* and *para* isomers but not for the *meta* derivative where the SBF critical energy is too high to be counterbalanced by the looseness of the transition structure. As a consequence, in a 0- to 6-eV internal energy range, *k*(SBF) is always lower than *k*(RER) and the ratio of peaks intensities [SBF]/[RER] lower than unity for the *meta* isomers.

It may be noted that this *meta* effect would be also expected for π-donor substituents other than OH or OCH_3. Accordingly, this effect also appears with donor substituents such as NH_2 or with alkyl chains different from *n*-alkyl groups as exemplified in the last lines of Table 1.

Finally, the importance of the *meta* effect in the analytical aspect of mass spectrometry should be underlined. It provides a useful means to distinguish this isomer in complicated mixtures as recently evidenced in lacquer samples and pyrolysis products of lignins and polyphenols.[33]

REFERENCES

[1] see for example: a) F. Turecek. The McLafferty and Related Rearrangements in N.M.M. Nibbering. In The Encyclopedia of Mass Spectrometry, Vol. *4*, M. L. Gross, R. M. Caprioli (Eds), Fundamentals of and Applications to Organic (and Organometallic compounds). Elsevier: Amsterdam, The Netherlands, **2005**, 396–403. b) T. Baer, B. Sztaray. The Statistical Theory for Unimolecular Decay of Organic and Organometallic Ions in N.M.M. Nibbering. In The Encyclopedia of Mass Spectrometry Vol. *4*, M. L. Gross, R. M. Caprioli (Eds), Fundamentals of and Applications to Organic (and Organometallic compounds). Elsevier: Amsterdam, The Netherlands, **2005**, 9–18. c) D. Kuck. Structures and Properties of Gas-Phase Organic Ions Radical Cations, Overview in N.M.M. Nibbering. In The Encyclopedia of Mass Spectrometry Vol. *4*, M. L. Gross, R. M. Caprioli (Eds), Fundamentals of and Applications to Organic (and Organometallic compounds). Elsevier: Amsterdam, The Netherlands, **2005**, 97–115. d) D. Kuck. Tropylium and Related Ions in N.M.M. Nibbering. In The Encyclopedia of Mass Spectrometry Vol. *4*, M. L. Gross, R. M. Caprioli (Eds), Fundamentals of and Applications to Organic (and Organometallic compounds), Elsevier: Amsterdam, The Netherlands, **2005**, 199–214.

[2] E. S. Mukhtar, I. W. Griffiths, F. M. Harris, J. H. Beynon. Photodissociation of mass-selected ions investigated using a modified ZAB—2F spectrometer. *Int. J. Mass Spectrom. Ion Phys.* **1981**, *37*(2), 159–166.

[3] I. W. Griffiths, E. S. Mukhtar, F. M. Harris, J. H. Beynon. Comparison of photo-excitation of ions and collisional excitation using gases. *Int. J. Mass Spectrom. Ion Phys.* **1981**, *39*(2), 125–132.

[4] I. W. Griffiths, E. S. Mukhtar, F. M. Harris, J. H. Beynon. The effect of source temperature on the average internal energy of positive ions. *Int. J. Mass Spectrom. Ion Phys.* **1982**, *43*(4), 283–292.

[5] J. H. Chen, J. D. Hays, R. C. Dunbar. Competitive two-channel photodissociation of n-butylbenzene ions in the Fourier transform ion cyclotron resonance mass spectrometer. *J. Phys. Chem.* **1984**, *88*(20), 4759–4764.

[6] M. J. Welch, D. J. Pereles, E. White. Photodissociation of the molecular ion of n-butylbenzene: effect of photon energy. *Org. Mass Spectrom.* **1985**, *20*(6), 425–426.

[7] T. Baer, O. Dutuit, H. Mestdagh, C. Rolando. Dissociation dynamics of n-butylbenzene ions: the competitive production of *m/z* 91 and *m/z* 92 fragment ions. *J. Phys. Chem.* **1988**, *92*(20), 5674–5679.

[8] S. T. Oh, J. C. Choe, M. S. Kim. Photodissociation dynamics of n-butylbenzene molecular ion. *J. Phys. Chem.* **1996**, *100*(32), 13367–13374.

[9] O. K. Yoon, W. G. Hwang, J. C. Choe, M. S. Kim. Internal energy content of n-butylbenzene, bromobenzene, iodobenzene and aniline molecular ions generated by two-photon ionization at 266 nm. A photodissociation study. *Rapid Comm. Mass Spectrom.* **1999**, *13*(7), 1515–1521.

[10] A. G. Harrison, M. S. Lin. Energy dependence of the fragmentation of the *n*-butylbenzene molecular ion. *Int. J. Mass Spectrom. Ion Phys.* **1983**, *51*(2–3), 353–356.

[11] S. Nacson, A. G. Harrison. Energy transfer in collisional activation. Energy dependence of the fragmentation of *n*-alkylbenzene molecular ions. *Int. J. Mass Spectrom. Ion Processes* **1985**, *63*(2–3), 325–337.

[12] S. A. McLuckey, L. Sallans, R. B. Cody, R. C. Burnier, S. Verma, B. S. Freiser, R. G. Cooks. Energy-resolved tandem and fourier-transform mass spectrometry. *Int. J. Mass Spectrom. Ion Phys.* **1982**, *44*(3–4), 215–229.

[13] S. A. McLuckey, C. E. D. Ouwerkerk, A. J. H. Boerboom, P. G. Kistemaker. The effect of collision energy in polyatomic ion/neutral target collisions over a range of 10–6000 eV. *Int. J. Mass Spectrom. Ion Processes* **1984**, *59*(1), 85–101.

[14] F. Muntean, P. B. Armentrout. Modeling kinetic shifts and competition in threshold collision induced dissociation. Case study: n-butylbenzene cation dissociation. *J. Phys. Chem. A* **2003**, *107*(38), 7413–7422.

[15] A. I. Fernandez, A. A. Viggiano, J. Troe. Two-channel dissociation of chemically and thermally activated n-butylbenzene cations. *J. Phys. Chem. A* **2006**, *110*(27), 8467–8476.

[16] R. C. Dunbar, R. Klein. Spectroscopy of radical cations. The McLafferty rearrangement product in fragmentation of n-butylbenzene and 2-phenylethanol ions. *J. Am. Chem. Soc.* **1977**, *99*(11), 3744–3746.

[17] R. G. McLoughlin, J. D. Morrison, J. C. Traeger. A photoionization study of the $[C_7H_8]^{·+}$ ion formed from some monosubstituted alkyl benzenes. *Org. Mass Spectrom.* **1978**, *13*(8), 483–485.

[18] P. C. Burgers, J. K. Terlouw, K. Levsen. Gaseous $[C_7H_8]^{·+}$ ions: [methylene cyclohexadiene].$^+$ a stable species in the gas phase. *Org. Mass Spectrom.* **1982**, *17*(6), 295–298.

[19] M. Rabrenović, A. G. Brenton, T. Ast. A study of $[C_7H_8]^{·+}$ $^{\text{and}}$ $[C_7H_8]^{2+}$ ions formed from different precursor molecules. *Org. Mass Spectrom.* **1983**, *18*(12), 587–595.

[20] R. G. McLoughlin, J. D. Morrison, J. C. Traeger. Photoionization of the C-1-C-4 monosubstituted alkyl benzenes: thermochemistry of $[C_7H_7]^+$ and $[C_8H_9]^+$ formation. *Org. Mass Spectrom.* **1979**, *14*(1), 104–108.

[21] J. Troe, V. G. Ushakov, A. A. Viggiano. On the model dependence of kinetic shifts in unimolecular reactions: the dissociation of the cations of benzene and n-butylbenzene. *J. Phys. Chem. A* **2006**, *110*(4), 1491–1499.

[22] S. Halbert, G. Bouchoux. Isomerization and dissociation of n-butylbenzene radical cation. *J. Phys. Chem. A* **2012**, *116*(4), 1307–1315.

[23] Gaussian 03, Revision B. 04, Gaussian, Inc., Pittsburgh, PA, **2003**.

[24] a) K. E. Riley, B. T. Op't Holt, K. M. Merz Jr. Critical assessment of the performance of density functional methods for several atomic and molecular properties. *J. Chem. Theor. Comput.* **2007**, *3*(2), 407–433. b) S. F. Sousa, P. A. Fernandes, M. J. Ramos. General performance of density functionals. *J. Phys. Chem. A* **2007**, *111*(42), 10439–10452. c) J. Tirado-Rives, W. L. Jorgensen. Performance of B3LYP density functional methodsfor a large set of organic molecules. *J. Chem. Theor. Comput.* **2008**, *4*(2), 297–306. d) L. Rao, H. Ke, G. Fu, X. Xu, Y. Yan. Performance of several density functional theory methods on describing hydrogen bond interactions. *J. Chem. Theor. Comput.* **2009**, *5*(1), 86–96.

[25] a) L. A. Curtiss, K. Raghavachari, P. C. Redfern, V. Rassolov, J. A. Pople. Gaussian-3 (G3) theory for molecules containing first and second-row atoms. *J. Chem. Phys.* **1998**, *109*(18), 7764–7776. b) A. Baboul, L. A. Curtiss, P. C. Redfern, K. Raghavachari. Gaussian-3 theory using density functional geometries and zero-point energies. *J. Chem. Phys.* **1999**, *110*(16), 7650–7657. c) L. A. Curtiss, P. C. Redfern, K. Raghavachari, V. Rassolov, J. A. Pople. Gaussian-3 theory using reduced Moller-Plesset order. *J. Chem. Phys.* **1999**, *110*(10), 4703–4709.

[26] a) Y. Kamiya, T. Miyakoshi. Synthesis of urushiol components and analysis of urushi sap from Rhus vernicifera. *J. Oleo Sci.* **2001**, *50*(11), 865–874. b) Y. Kamiya, W. Saito, T. Miyakoshi. Synthesis and identification of Laccol components from Rhus succedanea lacquer sap. *J. Oleo Sci.* **2002**, *51*(7), 473–483.

[27] a) N. Maras, S. Polanc, M. Koc var. Microwave-assisted methylation of phenols with tetramethylammonium chloride in the presence of K_2CO_3 or Cs_2CO_3. *Tetrahedron* **2008**, *64*(51), 11618–11624. b) N. Kataoka, Q. Shelby, J. P. Stambuli, J. F. Hartwig. Air stable, sterically hindered ferrocenyl dialkylphosphines for palladium-catalyzed C–C, C–N, and C–O bond-forming cross-couplings. *J. Org. Chem.* **2002**, *67*(16), 5553–5566. c) A. Krasovskiy, C. Duplais, B. H. Lipshutz. Zn-Mediated, Pd-Catalyzed Cross-Couplings in Water at Room Temperature Without Prior Formation of Organozinc Reagents. *J. Am. Chem. Soc.* **2009**, *131*, 15592–15593.

[28] a) F. Alonso, P. Candela, C. Gomez, M. Yus. The $NiCl_2$-Li-arene (cat.) combination as reducing system, part 9: Catalytic hydrogenation of organic compounds using the $NiCl_2$-Li-(Naphthalene or polymer-supported naphthalene) (cat.) combination. *Adv. Synth. Catal.* **2003**, *345*(1–2), 275–279. b) J. Tateiwa, E. Hayama, T. Nishimura, S. Uemura. Metal cation-exchanged montmorillonite (Mn + −mont)-catalysed aromatic alkylation with aldehydes and ketones. *J. Chem. Soc. Perkin Trans. 1* **1997**, *13*, 1923–1928. P. E. Cross, R. P. Dickinson, J. E. G. Kemp, P. R. Leeming, L. G. Pullman. Compounds with gastric antisecretory activity. 1. Phenoxyalkylamines. *J. Med. Chem.* **1977**, *20*(10), 1317–1323. M. A. Elsohly, M. A. Elsohly, D. A. Benigni, E. S. Watson, T. L. Little Jr. Analogs of poison Ivy urushiol – Synthesis and biological-activity of disubstituted normal alkylbenzenes. *J. Med. Chem.* **1986**, *29*(5), 606–611.

[29] a) R. B. Bates, T. J. Siahaan, K. Suvannachut. A new rearrangement of alkoxybenzyl anions. *J. Org. Chem.* **1990**, *55*(4), 1328–1334. b) I. Ujváry, G. Mikite. A practical synthesis of 3-n-propylphenol, a component of tsetse fly attractant blends. *Org. Process Res. Dev.* **2003**, *7*(4), 585–587. c) H. P. Tyman, S. K. Mehet. The separation and synthesis of lipidic 1,2-and 1,3-diols from natural phenolic lipids for the complexation and recovery of boron. *Chem. Phys. Lipids* **2003**, *126*(2), 177–199. K. Takaishi, Y. Alen, K. Kawazu. Synthesis and antinematodal activity of 3-n-alkylphenols. *Bio. Biotechnol. Biochem.* **2004**, *68*(11), 2398–2400. J. H. P. Tyman, S. J. A. Iddenten. The synthesis of oxime reagents from natural and semi-synthetic phenolic lipid and alkanoic acid resources for the solvent recovery of copper(II). *J. Chem. Technol. Biotechnol.* **2005**, *80*(11), 1319–1328.

[30] E. P. Hunter, S. G. Lias. Standard reference database no. 69. NIST Chemistry Webbook; National Institute of Standards and Technology: Gaithersburg, MD, **2005**. http://webbook.nist.gov/chemistry/

[31] J. Cioslowski. A new population analysis based on atomic polar tensors. *J. Am. Chem. Soc.* **1989**, *22*, 8333–8336.

[32] G. Bouchoux. Heats of formation and protonation thermochemistry of gaseous benzaldehyde, tropone and quinone methides. *Chem. Phys. Lett.* **2010**, *495*, 192–197.

[33] A.-S. Le Hô, M. Regert, O. Marescot, C. Duhamel, J. Langlois, T. Miyakoshi, C. Genty, M. Sablier. Molecular criteria for discriminating museum Asian lacquerware from different vegetal origins by pyrolysis gas chromatography/mass spectrometry. *Anal. Chim. Acta* **2012**, *710*, 9–16.